

$$E(p, a, b) = \int \frac{dp}{(p+a)(p-b)^2} \\ = \frac{1}{(a+b)^2} \ln \left( \frac{p+a}{p-b} \right) - \frac{1}{(a+b)(p-b)} \quad (13b)$$

Now, the integral  $I(t)$  can be written as

$$I(t) = \frac{K(\gamma+1)^2}{4\gamma(b_1-b_0)} \left[ \frac{b_1}{(p-b_1)(p^2-a^2)} - \frac{b_0}{(p-b_0)(p^2-a^2)} \right. \\ \left. + \frac{b_1}{2a} \{E(p, -a, b_1) - E(p, a, b_1)\} \right. \\ \left. - \frac{b_0}{2a} \{E(p, -a, b_0) - E(p, a, b_0)\} \right] \quad (14)$$

In particular, when the integration is from the blunt leading edge, the lower limits  $X_1$  and  $t_1$  in Eq. (8) are zero, and  $X = I(t)$ . The leading edge solution for  $X \rightarrow 0$  is obtained by expanding Eq. (14) for  $p \gg 1$  and the result for the pressure is

$$P(X \rightarrow 0) \approx [2/9 \cdot \gamma(\gamma+1)K^2]^{1/3} X^{-2/3}$$

### Results and Discussions

The closed-form solution given by Eq. (14) was solved for different values of the incidence parameter  $M_\infty \theta$  and the results are compared with Cheng's theory in Fig. 1. The values of  $X$  were obtained by calculating the integral  $I$  for different values of  $P (= K/t)$ . For each value of  $M_\infty \theta$ , there is a different downstream limit corresponding to the wedge value. Far downstream, Cheng's theory predicts an undershoot in pressure and a subsequent oscillatory approach to the downstream. Recently Cheng and Kirsch<sup>9</sup> have given a higher-order theory which almost removes the undershoot and predicts close agreement with the wedge value downstream.

Since the pressure area relation Eq. (2) is valid only in the limit of  $\gamma \rightarrow 1$ , in order to give good agreement with experimental results, Kemp suggested the following modification to Cheng's pressure area relation (Eq. 2)

$$p_e [y_s - (\gamma+1)/2 \cdot y_b] = (\gamma-1)/2 \cdot D_N \quad (15)$$

where  $y_s$  is the shock waveshape. When the leading edge is sharp, Eq. (15) reduces to the oblique shock theory result  $y_s = (\gamma+1)/2 \cdot y_b$  for  $M_\infty \gg 1$ . For the case of blunt leading edge, to use tangent wedge approximation along with Eq. (15), we need one more relation between  $y_s$  and the effective body shape  $y_e$ . For large  $M_\infty$ , it is reasonable to assume  $(\gamma+1)/2 \cdot y_e$  and the dotted line in Fig. 1 shows the results with these modifications.

For large  $M_\infty \theta$ , the solution can be obtained in a simpler form than Eq. (14) by approximating the tangent wedge rule as  $P = (\gamma+1)/2 \cdot M_\infty^2 \theta^2$ . This gives after integration the closed-form solution for the pressure

$$-(\gamma+1)/4 \cdot \zeta = \lambda + (\lambda^2/2) + \ln(1-\lambda) \quad (16) \\ \zeta = \frac{4\theta^3 x}{(\gamma-1)C_{DN} t_e} \\ \lambda = \left( \frac{\gamma+1}{2} \cdot \frac{\gamma M_\infty^2 \theta^2}{P} \right)^{1/2}$$

Though the solution (16) is valid for  $M_\infty \theta \gg 1$ , it is found to be quite accurate even for moderate values. For  $M_\infty \theta = 1$  and  $P = 28$ , the values of  $(2\theta^3 \kappa / \epsilon C_{DN} t_e)$  calculated by two Eqs. (14) and (16) differ only by 4%.

### References

- Cheng, H. K., Hall, J. G., Golian, T. C., and Hertzberg, A., "Boundary-layer Displacement and Leading Edge Bluntness Effects in High Temperature Hypersonic Flows," *Journal of Aerospace Science*, Vol. 28, No. 5, May 1961, pp. 353-381.

<sup>2</sup>Chernyi, G. G., "Effect of Slight Blunting of Leading Edge of an Immersed Body on the Flow around it at Hypersonic Speeds," TT F-35, 1960, NASA.

<sup>3</sup>Hayes, W. D. and Probstein, R. F., "Hypersonic Flow Theory," *Inviscid Flows*, Vol. I, Academic Press, New York, 1966, p. 364.

<sup>4</sup>Schnieder, W., "Asymptotic Behavior of Hypersonic Flow over Blunted Slender Wedges," *AIAA Journal*, Vol. 6, No. 11, Nov. 1968, pp. 2235-2236.

<sup>5</sup>Stollery, J. L., "Hypersonic Viscous Interaction on Curved Surfaces," *Journal of Fluid Mechanics*, Vol. 43, Pt. 3, 1970, pp. 497-511.

<sup>6</sup>Stollery, J. L., Pimputkar, S., and Bates, L., "Hypersonic Viscous Interaction," *Fluid Dynamic Transactions*, Vol. 6, Pt. II, 1971, pp. 545-562.

<sup>7</sup>Murthy, A. V., "Studies in Hypersonic Viscous Interactions," Ph.D. thesis, Dec. 1972, Dept. of Aerodynamics, Cranfield Institute of Technology, Bedford, England.

<sup>8</sup>Kemp, J. H., "Hypersonic Viscous Interaction on Sharp and Blunt Inclined Flat Plates," *AIAA Journal*, Vol. 7, No. 7, July 1969, pp. 1280-1289.

<sup>9</sup>Cheng, H. K. and Kirsch, J. W., "On the Gas Dynamics of an Intense Explosion with an Expanding Contact Surface," *Journal of Fluid Mechanics*, Vol. 39, Pt. 2, 1969, pp. 289-305.

## Subsonic Flow into a Downstream Facing Inlet

Theo G. Keith Jr.\*

The University of Toledo, Toledo, Ohio

BY changing the direction on the internal engine flow, through the use of a variable pitch fan, reverse thrust can be generated in a fan engine. However, in accomplishing a thrust reversal by this method, flow will be taken into the propulsor from its downstream opening and thus the exhaust nozzle will function as an inlet. Since the nozzle was not necessarily intended to be used in this fashion, it is of interest to examine expected performance characteristics. As a first step, a simple extension of an earlier study by Fradenburg and Wyatt, Ref. 1, is used in this note to estimate the total pressure recovery of the inlet as a function of the freestream Mach number for parametric values of the inlet or duct Mach number.

The flow model assumes that the nozzle can be represented as a sharp-lip cylindrical duct facing in the downstream direction, and that the internal duct flow is separated due to the fact that the flow cannot turn the 180° required to stay attached to the duct wall. Because of this, the total pressure does not remain constant throughout the flow field.

Since the analysis closely follows that presented in Ref. 1, only the major points will be brought out herein. A mass-momentum balance on a control volume drawn around the inlet results in the following two expressions:

Received January 14, 1974. This work was performed while the author was an ASEE summer faculty fellow at the NASA Lewis Research Center.

Index categories: Aircraft Deceleration Systems; Subsonic and Transonic Flow.

\*Assistant Professor, Dept. of Mechanical Engineering. Member AIAA.

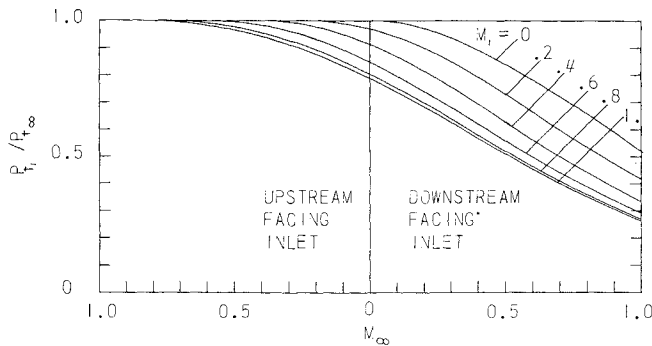


Fig. 1 Total pressure recovery vs freestream mach number for various inlet mach numbers.

$$(A_1/A_{\infty}) = (M_{\infty}/M_1)(P_{\infty}/P_1) \left( \frac{T_1}{T_{\infty}} \right)^{1/2} \quad (1)$$

$$\Phi_1 + \Phi_{\infty} = 0 \quad (2)$$

where  $A$  is the area,  $M$  the Mach number,  $P$  the static pressure,  $T$  the static temperature, and  $\Phi$  the momentum parameter equal to:  $[(P - P_{\infty}) + \gamma PM^2] A$ . Also, subscript 1 refers to a location within the inlet where the flow is uniform and subscript  $\infty$  denotes an external uniform flow location far upstream of the inlet. It should be mentioned that Eq. (2) is based on the assumption that intake lip is sharp and therefore cannot support a suction force and that the pressure integral over the control surface vanishes for reasons detailed in Ref. 1.

When the area ratio is eliminated between Eqs. (1) and (2), and use is made of the stagnation property relations for temperature and pressure, we obtain

$$\frac{P_{t1}}{P_{t\infty}} = \frac{\left( \frac{1 + \frac{\gamma-1}{2} M_1^2}{1 + \frac{\gamma-1}{2} M_{\infty}^2} \right)^{\frac{\gamma+1}{2(\gamma-1)}}}{(1 + \gamma M_1^2) \left( \frac{1 + \frac{\gamma-1}{2} M_{\infty}^2}{1 + \frac{\gamma-1}{2} M_1^2} \right)^{1/2} + \gamma M_1 M_{\infty}} \quad (3)$$

Thus the total pressure recovery,  $P_{t1}/P_{t\infty}$ , is a function of just the freestream and duct Mach numbers. In addition, it can be seen that the direction of the freestream flow affects the magnitude of the recovery only through the  $\gamma M_1 M_{\infty}$  term. Figure 1 is the graph of the expression. Notice that pressure recoveries found from values of  $M_{\infty}$  to the right of the origin correspond to an upstream facing intake. Total pressure ratios are much lower in the downstream facing duct case. Furthermore, the maximum total pressure, for a given duct Mach number, that can be recovered with a rear facing sharp-lip inlet occurs as the freestream Mach number approaches zero. When  $M_{\infty} = 0$ , (static case), the total pressure recovered equals the free-stream static pressure,  $P_{\infty}$ . Thus at best, there is a complete loss of the freestream dynamic head.

Finally, it should be pointed out that type of inlet considered in this note produces a larger total pressure loss than would occur in a variable area or flared inlet, which is a physically more realistic intake. On the other hand, a well rounded inlet, which is clearly not a practical exhaust nozzle when the propulsion unit is used to develop forward thrust, is capable of complete total pressure recovery. Thus the actual intake experiences total pressure losses somewhere between those predicted here and unity.

However, since reverse thrust applications occur at low Mach numbers and therefore at the largest values of pressure recovery, these differences should not be unreasonable.

#### References

- <sup>1</sup>Fradenburg, E. A. and Wyatt, D. D., "Theoretical Performance Characteristics of Sharp-Lip Inlets," TN 3004, 1953 NACA.

## Cavity Growth and Collapse Phase of Hydraulic Ram

G. C. Cardea\* and P. J. Torvik†

Air Force Institute of Technology, Wright-Patterson Air Force Base, Ohio

#### Introduction

WHEN a projectile traveling at a high rate of speed encounters a liquid-filled container, several mechanisms contribute to the generation of high pressures within the liquid. The generation of these large pressures is referred to as the hydraulic ram phenomenon.<sup>1</sup> Such high pressures may cause the growth of cracks emanating from the entrance or exit hole and lead to rupture of a tank wall. High internal pressures also may cause bulging of tank walls and damage to the supporting structure. Finally, any equipment inside the container may be damaged by high pressure.

Several mechanisms can lead to the generation of pressures large enough to produce damage. As the projectile strikes and penetrates the entrance wall, a strong shock wave will be driven into the fluid. This phenomenon has been the subject of a number of studies.<sup>2,3</sup> As the projectile moves through the fluid, a pressure field is generated around the projectile. This phase of the process, which is made quite complex by the tumbling which typically occurs when projectiles pass through liquids, has been considered quite extensively.<sup>1</sup> The third phase, the subject of the present study, is the generation of pressures due to the formation and collapse of the cavity which forms behind the projectile. It has been noted previously that such cavities will form, will generate pressures, and are loosely analogous to cavities formed by underwater explosions.<sup>1</sup>

It is the purpose of this note to show that the formulae developed for the purpose of analyzing underwater explosions can be adapted to projectile penetration and used to predict the relationships between the period of the cavity growth and collapse cycle, the energy required to produce the cavity, the maximum size of the cavity, and the peak pressures generated by its collapse. Some experimental data are used to confirm the applicability of such predictions.

Received January 15, 1974. Based on a thesis submitted in partial fulfillment of the requirements for the Master of Science degree. We are indebted to C. C. Gebhard of the Air Force Flight Dynamics Laboratory for allowing us to use his unpublished experimental data.

Index categories: Aircraft Fuels and Fuel Systems; Aircraft Structural Design (Including Loads); Military Aircraft Missions.

\*Presently Flight Test Engineer, Edwards Air Force Base, Calif.

†Professor of Mechanics.